

Article

# High-Frequency Dependence of Acoustic Properties of Three Typical Sediments in the South China Sea

Jingqiang Wang<sup>1</sup>, Zhengyu Hou<sup>2,3,\*</sup>, Guanbao Li<sup>1,4</sup>, Guangming Kan<sup>1,4</sup>, Baohua Liu<sup>4,5</sup>, Xiangmei Meng<sup>1,4</sup>, Qingfeng Hua<sup>1</sup> and Lei Sun<sup>1</sup>

<sup>1</sup> Key Laboratory of Marine Geology and Metallogeny, First Institute of Oceanography, MNR, No. 6 Xianxialing Road, Qingdao 266061, China

<sup>2</sup> School of Ocean Engineering and Technology, Sun Yat-sen University, Zhuhai 519000, China

<sup>3</sup> Key Laboratory of Ocean and Marginal Sea Geology, Key Laboratory of Science and Technology on Operational Oceanography, South China Sea Institute of Oceanology, Chinese Academy of Sciences, Guangzhou 510301, China

<sup>4</sup> Laboratory for Marine Geology, Qingdao National Laboratory for Marine Science and Technology, No. 1 Wenhai Road, Jimo City, Qingdao 266237, China

<sup>5</sup> National Deep Sea Center, Ministry of Natural Resources (MNR), No. 1 Weiyang Road, Jimo City, Qingdao 266237, China

\* Correspondence: zzhou2022@163.com

**Abstract:** The acoustic characteristics of three fine-grained sediments (silty sand, silt, silty clay) in the South China Sea (SCS) were measured and analyzed at high frequency range of 27–247 kHz. The measurement results show that the sound speed dispersion is a positive linear relation at the measured frequency range, and the attenuation follows nonlinear frequency dependence,  $\alpha = kf^n$ , where  $n$  ranges from 0.59 to 0.85 for the three different sediments in the SCS. The frequency dependence of sound speed and attenuation were compared with the published literature. It was found that for silty clay, clayey silt, silt, and silty sand, the dispersion characteristics of these four sediments are basically consistent; in general, the dispersion of coarse particles is significant, and that of fine particles is weak, and permeability is the key parameter that determines the inflection point of high frequency to low frequency. By modeling these sediments with the Biot–Stoll model, it was found that the Biot–Stoll model can better predict the frequency-dependent characteristics of sound attenuation in a high-frequency band under the matching constraints of sound speed dispersion characteristics, indicating that the Biot–Stoll model has good applicability to different types of sediments in a high-frequency band.

**Keywords:** sediment acoustic; frequency dependence; sound speed; attenuation; Biot–Stoll model



**Citation:** Wang, J.; Hou, Z.; Li, G.; Kan, G.; Liu, B.; Meng, X.; Hua, Q.; Sun, L. High-Frequency Dependence of Acoustic Properties of Three Typical Sediments in the South China Sea. *J. Mar. Sci. Eng.* **2022**, *10*, 1295. <https://doi.org/10.3390/jmse10091295>

Academic Editor: Anabela Oliveira

Received: 7 July 2022

Accepted: 11 August 2022

Published: 14 September 2022

**Publisher's Note:** MDPI stays neutral with regard to jurisdictional claims in published maps and institutional affiliations.



**Copyright:** © 2022 by the authors. Licensee MDPI, Basel, Switzerland. This article is an open access article distributed under the terms and conditions of the Creative Commons Attribution (CC BY) license (<https://creativecommons.org/licenses/by/4.0/>).

## 1. Introduction

Seafloor sediment is a kind of solid-liquid two-phase medium, mainly composed of solid particles and pore fluid. The acoustic propagation characteristics of seafloor sediments have been an important research topic in hydro-acoustics, geophysics, and other disciplines [1,2].

As early as in the 1950s, Gassmann (1951) first proposed the Gassmann theory, which can quantitatively reflect the relationship between velocity and porosity [3]. In 1956, Biot described a three-variable model of porous solids and free and trapped fluids based on the theory with mass coupled terms [4]. Subsequently, Biot developed Gassmann's theory of a fluid-saturated porous two-phase medium based on the potential characteristics of moist soil and the absorption characteristics of acoustic waves, which laid the foundation of the wave theory of two-phase media. The Biot theory fully considers the dual-phase characteristics of porous media, discovers the second type of longitudinal waves (slow p-waves), and points out that the relative motion in pore fluid controlled by viscous force

is an important mechanism for the attenuation of elastic waves during the propagation of porous media.

The Biot theory indicates that the significant frequency band of sound speed dispersion in water-saturated sediments is 1–10 kHz. At low frequencies, attenuation is proportional to the square of frequency; at high frequencies, attenuation is proportional to the square root of the frequency. Hamilton gave an empirical formula for the sound speed and attenuation of seafloor sediments and sediment type and frequency, and he pointed out that the sound speed dispersion is very weak and can be ignored [5]; in the frequency range from a few hertz to megahertz, the attenuation is approximately proportional to the frequency. However, a large number of subsequent sampling measurements and in situ measurement experiments show that the sound speed also has a dispersion phenomenon.

Subsequently, Stoll applied the Biot theory to seafloor sediments and established the Biot–Stoll model [6], which considered that the solid particles in the sediment were attached to the pore water as an elastic “frame” and introduced the frame loss. Compared with the fluid model and the viscoelastic model, the model predicts the sound speed and attenuation coefficient in the sandy sediment more accurately and can better describe the characteristics of sound speed dispersion. Williams (2001) developed the effective density fluid model (EDFM) model, considering that the frame moduli are far smaller than the grain moduli and the fluid moduli [7], and if the frame moduli can be set to zero, the sediment is approximated as a fluid medium represented by an equivalent density, which reduces the 13 parameters involved in the Biot–Stoll model to 9; and in soft sediments, such as mud or fine sand, the reflection losses predicted by the EDFM model agree well with the Biot–Stoll model.

Considering the widespread attenuation, the Biot theory has received in the seafloor acoustics field, relatively little has been reported regarding conform of its validity [8]. Hovem and Ingram [9] used glass beads in their experiments and showed that in the frequency range 20–300 kHz the results are good agreement with the Biot theory. Simpson et al. [10] reported the field measurements of sandy sediments supporting the Biot theory over the 3–80 kHz frequency band. The measurements results appear consistent with the Biot model, but attenuation is essentially a linear frequency dependence in the measurement frequency band. In the SAX99 offshore experiment [1], the sound speed of sandy sediments in the 125–400 kHz frequency band and the attenuation of sandy sediments in the 2.6–400 kHz frequency band were obtained using an in-situ system, and the results showed that the sound speed dispersion in the frequency range from 25 to 100 kHz is weak, which is consistent with the Biot theory; the attenuation is approximately linear with the frequency, and the deviation above 50 kHz deviates from the Biot theory. Ragione et al. [11] reported a study based upon a micro-mechanics analysis to support the presence of both slow and fast compression waves in different materials. Buckingham [12] developed the viscous grain shearing model (VGS) based on grain-to-grain contacts in sediments. The VGS model has been used to compare with the Biot theory. The major feature of the Biot theory in the high-frequency band is to predict the frequency dependence of the sound speed and attenuation [13] (Bonomo and Isakson, 2018). Holmes et al. [14] reviewed a large number of attenuation data, arguing that the attenuation of sandy sediments varies with frequency. Sesarego et al. [15] measured the sound speed and attenuation of sandy sediments in the 0.5 to 1.3 MHz frequency band in a laboratory setting. Attenuation varies nonlinearly with frequency and sound speed, and attenuation data are inconsistent with the Biot theory, possibly caused by solid particle volumetric scattering. Yu et al. [16] obtained the sound speed and attenuation of fine sand in the 90–170 kHz frequency band in a laboratory water tank. The results showed that the sound speed dispersion of the sand sample is very weak, and consistent with the Biot–Stoll model, and the attenuation is approximately proportional to  $f^{0.35}$ , but higher than that predicted by the model, possibly due to the additional sound attenuation caused by the internal inhomogeneity of the sediment samples. The above studies focused on the coarse sediments, such as sandy sediment, but few studied on the fine-grained sediments acoustic properties.

In this paper, three fine-grained sediments in the South China Sea (SCS) were statistically analyzed, and their high-frequency acoustic properties were measured, and the high-frequency dependence of acoustic properties of the three sediments in the SCS was analyzed and compared using Biot–Stoll model.

## 2. Study Area and Method

In this paper, historical data of acoustic properties of seafloor sediments in the SCS are collected. The study area is located in the northern shelf and continental slope of the SCS, with a water depth ranging from 113 m to 1271 m. The northern continental shelf of the SCS is dominated by terrigenous clastic deposits, and there are four main types of sediments. Their distribution and characteristics are as follows: (1) Gravely sands are mainly distributed on the continental shelf south of the Pearl River Estuary, among which bioclasts are more common. (2) Sandy sediments are mainly distributed on the middle and outer continental shelves east of 116° E with a water depth of 50–200 m. This region has the characteristics of gradually thickening from west to east, and the sandy sediments near the 200 m water depth of the outer shelf front east of 113° E are the products of the early high-energy coastal zone. The rest are mainly distributed in the Beibu Gulf–Indochina Peninsula coastal estuary and the western and southwestern coastal shelf areas of Hainan Island. (3) Clay silt sediments are mainly distributed parallel to the coast. (4) The silty clay sediments are mainly distributed on the vast middle and outer continental shelves with a water depth of 50–200 m in the west of the Pearl River Estuary and are distributed in sheets or strips. The types of sediments in this area include silty clay, clay silt, silt, silty sand, sandy silt, and clay sand. From 2016 to 2018, the First Institute of Oceanography of the Ministry of Natural Resources and the South China Sea Institute of Oceanography of the Chinese Academy of Sciences carried out continuous measurement of the acoustic properties of seafloor sediments in the northern of the SCS. In this paper, three fine-grained sediments are selected to carry out high-frequency-dependent characteristic analysis, they are the sediment types with representative physical properties and obvious differences in the study area, including 37 stations of silty clay sediment samples, 31 stations of silty sediment samples, and 12 stations of silty sand sediment samples. All these sediments are collected by gravity sampler and acoustic properties are measured in the top 0.3 m of the sediment cores.

### 2.1. Laboratory Measurement Method

The whole measurement system consists of an acoustic measuring platform, a power amplifier, a self-developed acoustic transmitter/receiver instrument (ATRI), a prefilter amplifier, and transmitting and planar acoustic transducers with different frequencies. The ATRI is used to drive the transmitting transducer and receive the acoustic wave. The power amplifier is used to excite the transmitting acoustic signals. The prefilter amplifier is used to excite the receiving acoustic signals. The technical parameter of ATRI system is listed as follows:

- Number of acquisition channels: 2 channels;
- Sampling rate: up to 16 MHz, configurable by software;
- Sampling length: 10 ms;
- Sampling rate: 16 MHz;
- Resolution: 16 bit;
- Storage method: computer storage;
- Transmitting channel: 1 channel;
- Transmission frequency: 20 Hz~1 MHz, adjustable;
- Transmission waveform: sine wave, PCW, etc., the period is adjustable.

Before starting the measurement, all equipment was connected as shown in Figure 1 and place the sediment cores on the acoustic measuring platform. The sediment core length was measured with accuracy of  $\pm 0.1$  mm by the measuring platform, and the sound wave sampling rate was 16 MHz by the acoustic instrument, so that the accuracy of the sound

speed was estimated to be better than  $\pm 0.1\%$  for a typical sample with a length of 30 cm and the sound speed of 1500 m/s. The sound speed and attenuation were measured at the frequencies of 27, 51, 111, 214, and 247 kHz, respectively. The waveforms of sound signals at different frequencies recorded by the acoustic system are shown in Figure 2. The measurement was conducted in the standard condition (standard atmospheric pressure, 23°), and under the standard laboratory conditions the laboratory measurements can be correction to the in situ condition by using sound speed ratio method [17]. The details of the acoustic measurements can be found in Hou et al. [18] Section 2 and Figure 2.



Figure 1. Laboratory measurement system.

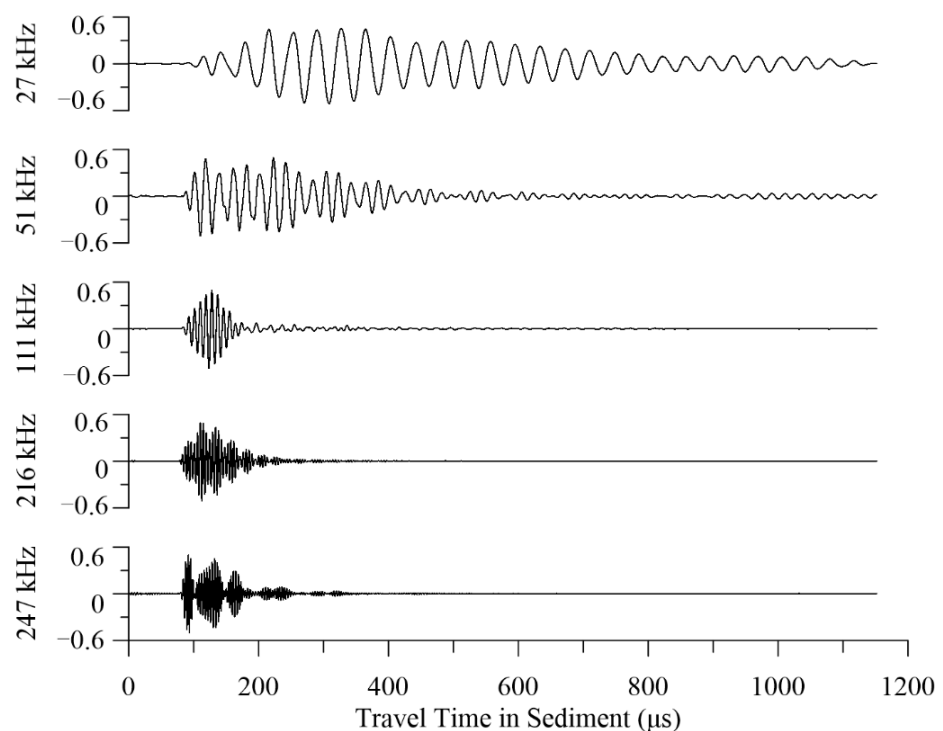


Figure 2. The waveforms of sound signals at different frequencies recorded by the acoustic system.

### 2.2. Biot–Stoll Model

In Biot–Stoll’s theory, sediment is regarded as a two-phase system composed of solid particles and pore water. Under the action of sound waves, the two displacements are different. Sediment particles are coupled with pore water as an elastic frame, and this coupling generates three types of wave fields from the interactions between the compression wave in the pore water, and the compression and shear wave in the elastic solid frame.

The Biot–Stoll model involves 13 parameters [19]: Porosity  $n$ , Grain bulk modulus  $K_g$ , Fluid dynamic viscosity  $\eta$ , Grain density  $\rho_s$ , Fluid density  $\rho_f$ , Fluid bulk modulus  $K_f$ , Permeability  $\kappa$ , Tortuosity  $\alpha$ , Pore size  $a$ , Dissipative Skeletal Bulk Modulus  $K_0$ , Dissipative Skeletal Shear Modulus  $\mu_0$ , Bulk dissipation factor  $\delta_k$ , and Shear dissipation factor  $\delta_\mu$ .

The longitudinal wave equation of Biot–Stoll is:

$$\nabla^2(H\varepsilon - C\zeta) = \frac{\partial^2}{\partial t^2}(\rho\varepsilon - \rho_f\zeta) \tag{1}$$

$$\nabla^2(C\varepsilon - M\zeta) = \frac{\partial^2}{\partial t^2}(\rho_f\varepsilon - m\zeta) - \frac{F\eta}{\kappa} \frac{\partial \zeta}{\partial t} \tag{2}$$

$$\varepsilon = \nabla \bullet \mathbf{u} \tag{3}$$

$$\zeta = n \nabla \bullet (\mathbf{u} - \mathbf{U}) \tag{4}$$

$$\rho = (1 - n)\rho_s + n\rho_f \tag{5}$$

where the  $\mathbf{u}$  and  $\mathbf{U}$  are the skeleton and pore fluid displacement vectors, respectively. The Biot elastic moduli  $\mathbf{H}$ ,  $\mathbf{C}$ , and  $\mathbf{M}$  are expressed as the bulk modulus of the framework, the bulk modulus of the pore fluid, and the bulk modulus of the particles, respectively:

$$\mathbf{H} = \frac{(K_g - K_b)^2}{D - K_b} + K_b + \frac{4\mu}{3} \tag{6}$$

$$\mathbf{C} = K_g \frac{(K_g - K_b)}{D - K_b} \tag{7}$$

$$\mathbf{M} = \frac{K_g^2}{D - K_b} \tag{8}$$

$$D = K_g \left[ 1 + n \frac{K_g}{K_f - 1} \right] \tag{9}$$

where  $K_b$  and  $\mu$  are Skeletal bulk modulus and shear modulus, which are complex constants:

$$K_b = K_b(1 + i\delta_k) \tag{10}$$

$$\mu = \mu_0(1 + i\delta_\mu) \tag{11}$$

The dispersion relations for the fast and slow waves corresponds to the roots of the following determinant system:

$$\begin{vmatrix} Hl^2 - \rho\omega^2 & \rho_f\omega^2 - Cl^2 \\ Cl^2 - \rho_f\omega^2 & m\omega^2 - Ml^2 - i\frac{\omega F\eta}{\kappa} \end{vmatrix} = 0 \tag{12}$$

$$l = l_r - j\alpha = \frac{\omega}{V} - j\alpha \tag{13}$$

$$\omega = 2\pi f \tag{14}$$

where  $l$  is the complex wave number. Once the roots of above equations are found, the compressional wave speed and attenuation can be expressed as:

$$V_p = \frac{1}{Re\sqrt{l_1}} \tag{15}$$

$$\alpha_p = -Im(l_1) \tag{16}$$

where  $l_1$  is the root with a negative imaginary component and the smaller real component.

### 3. Results and Discussion

#### 3.1. Measured Data

The average measured sound speed and attenuation at different frequencies for different sediment types including the ones from the three study areas are shown in Table 1. Figure 3 shows the sound speed dispersion of different sediments and the sound speed dispersion empirical formulas. The results show that the sound speed dispersion is a positive linear relation,  $V_p = kf + b$ , and the slope  $k$  changes with the sediment types and sedimentary environment. In SCS, the lowest slope is the silty clay sediment,  $k = 0.0658$ , and the highest slope is the silty sand,  $k = 0.0956$ . It is evident that in SCS, the slope  $k$  is related with the grain size, and when the grain size increased, the slope  $k$  increased. The slope  $k$  of clayey silt in Western Pacific (WP) is 0.0614, and the dispersion curve of WP has the similar trend with the SCS.

**Table 1.** The measured sound speed and attenuation at different frequencies.

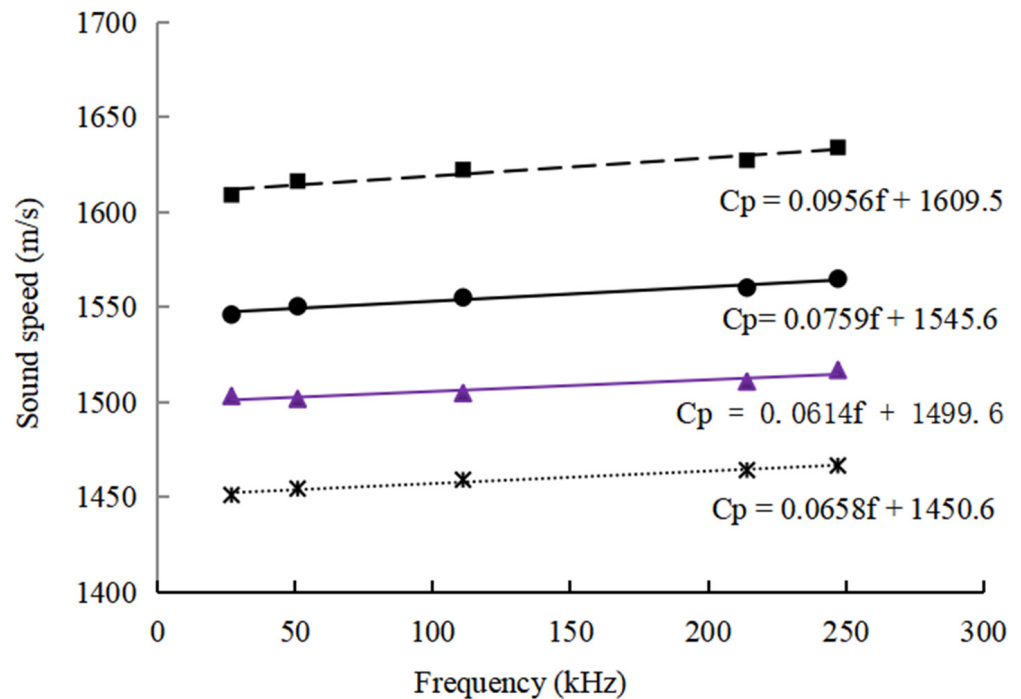
Study Area	Sediment Type	Range	Sound Speed (m/s)					Attenuation (dB/m)				
			27 kHz	51 kHz	111 kHz	214 kHz	247 kHz	27 kHz	51 kHz	111 kHz	214 kHz	247 kHz
South China Sea	Silty sand	Maximum	1641.13	1637.64	1643.92	1657.43	1671.05	29.99	42.01	59.24	78.71	112.05
		Minimum	1576.70	1586.23	1591.61	1586.86	1598.36	5.72	17.30	36.46	43.99	59.01
		Mean	1609.17	1616.43	1622.47	1627.38	1634.16	14.42	25.1	42.6	54.12	75.81
	Silt	Maximum	1568.66	1568.77	1574.62	1580.10	1583.05	27.9	35.0	37.14	51.7	75.5
		Minimum	1529.86	1527.96	1537.80	1539.12	1547.14	9.83	14.9	16.9	20.9	26.09
		Mean	1546.16	1550.56	1555.20	1560.32	1565.04	11.13	16.7	22.3	36.04	45.89
	Silty clay	Maximum	1461.18	1468.78	1469.51	1475.72	1474.19	6.06	18.5	24.52	40.6	65.87
		Minimum	1439.92	1442.96	1453.8	1453.74	1458.77	2.97	9.3	8.09	16.05	18.55
		Mean	1451.19	1454.56	1459.20	1464.30	1466.7	4.25	10.7	13.3	26.22	35.45
Western Pacific	Clayey silt	Maximum	1511.06	1512.11	1512.89	1515.71	1520.28	26.15	28.58	36.48	58.46	64.11
		Minimum	1495.53	1497.86	1499.06	1501.49	1505.79	18.19	22.58	28.91	34.15	39.19
		Mean	1503.28	1501.76	1504.08	1510.88	1516.96	22.38	24.21	33.57	42.36	49.59

The degree of dispersion is used to describe the frequency dispersion of sound velocity, defined as by subtracting the minimum from the maximum sound speed and then dividing by the minimum sound velocity. The dispersion curves of the SCS and WP sediments are almost parallel, the frequency dispersion degree of the four sediments is 1.0687% (silty clay), 1.0121% (clayey silt), 1.22% (silt), and 1.5529% (silty sand), respectively. From the slope  $k$  and dispersion degree, the SCS and WP sediments have little sound speed dispersion in the measured frequencies.

Williams et al. [1] believed that the grain modulus and porosity affect the sound speed dispersion over the frequency range, the permeability affects the sound speed dispersion in the middle frequency range from 10 kHz to 50 kHz, and the tortuosity affects the sound speed dispersion in the high frequency above 50 kHz. For our measurement frequency range, the four factors are all related with our measurement results, and the dispersion degree is a comprehensive reflection of these parameters. Figure 3 also shows that for silty clay, clayey silt, silt, and silty sand, the dispersion characteristics of these four sediments are basically consistent.

The tortuosity is closely related with the grain size, when the mean grain size is between 4 and 8 ( $\phi$ ), which is the average particle size of fine-grained sediment, the tortuosity is calculated by  $\alpha = -0.3 + 0.412 \phi$ ; that is to say, the tortuosity changes linearly with grain size. The average porosity of the four sediments (silty clay, clayey silt, silt, and silty sand) is 0.694, 0.663, 0.550, and 0.482, respectively, and the general trend is that

porosity gradually decreases with particle size. Although the mean grain size of silty clay and clayey silt is similar, the permeability of clayey silt is order of magnitude less than silty clay, which may be the reason why the dispersion characteristics of clayey silt are smaller than that of silty clay.



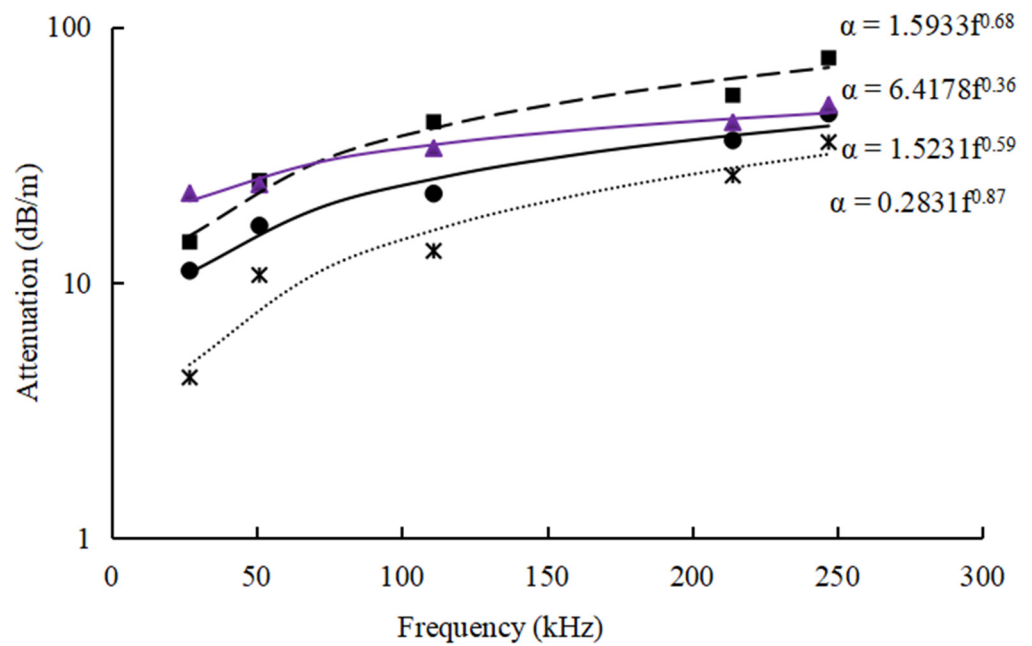
**Figure 3.** The sound speed dispersion of different sediments. The black ■ dots are silty sand, the black ● dots are silt, the black \* dots are silty clay in SCS, and the purple ▲ is clayey silt in WP.

Figure 4 shows the attenuation dispersion of different sediments and the attenuation dispersion empirical formulas. It is shown that the attenuation follows a power-law frequency dependence,  $\alpha = kf^n$ , and the  $n$  value of the four sediments is 0.35 (clayey silt), 0.59 (silt), 0.68 (silty sand), and 0.87 (silty clay), respectively. The attenuation of silty clay is the lowest in the four sediments, but the attenuation dispersion is the highest. Although silty clay in SCS and clayey silt in WP have similar particle size and porosity, their attenuation dispersion characteristics are quite different, the attenuation of clayey silt is the lowest in the four sediments ( $n = 0.35$ ). This phenomenon also shows that attenuation is affected by many factors, and sediment attenuation characteristics in different regions are different. Hamilton (1972) consistently maintained that the frequency dependence of attenuation in sediments obeys an  $f^1$  dependence, while according to the Biot–Stoll model, the attenuation coefficient deviates from a first-power dependence on frequency and varies as the square root of frequency ( $f^{1/2}$ ) at the high frequencies. According to our actual measurement results, attenuation is affected by many factors, such as the sediment types and sedimentary environment, and the attenuation frequency dependency is not strictly following  $f^1$  or  $f^{1/2}$  dependence. In this study, the  $n$  value of the three sediments in SCS changes from 0.59 to 0.87, while in WP, the  $n$  value of clayey silt is only 0.36.

### 3.2. Biot–Stoll Model Comparison

Seafloor sediments are composed of particles that form a solid skeleton, the voids between the units form pore spaces, and the pores are filled with fluids. This porous structure makes it very different from dense solid matter in many aspects such as mechanical properties and material state. The irregularity of the pore structure of the porous medium and the heterogeneity of the porous medium constitute the inhomogeneity of different types of sediments. This microscopic inhomogeneity causes the macroscopic physical

properties of the sediments to be very sensitive to slight changes in the pore fluid or pore structure. Therefore, when the sound wave propagates in the sediment, under its influence, the pores or fractures of the medium will be closed or opened, and the fluid in the pore spaces is moving relative to the elastic frame, resulting in changes in the macroscopic physical properties of the sediment, and resulting in changes in the speed of sound wave propagation, dissipation of energy, and attenuation of amplitude. The Biot–Stoll model involves 13 input parameters, and the true and accurate description of these parameters is the basis for describing the variation of the acoustic propagation characteristics of sediments and has far-reaching significance and great value for solving the general porous problem in practical applications.



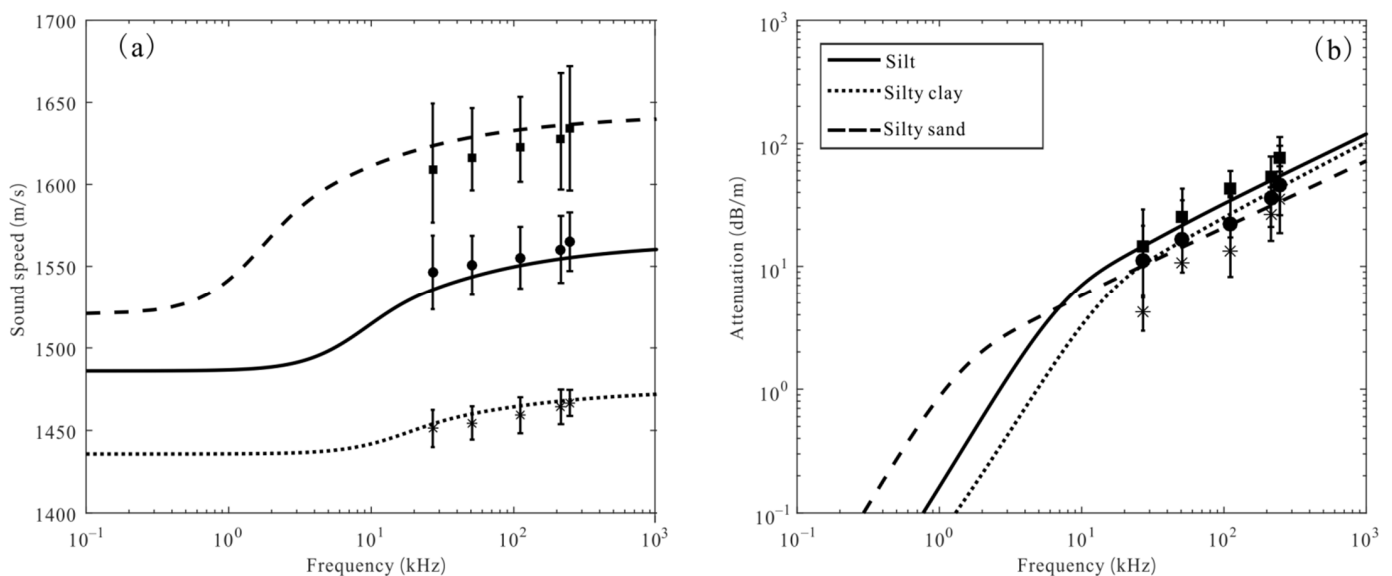
**Figure 4.** The attenuation dispersion of different sediments. The black ■ dots are silty sand, the black ● dots are silt, the black \* dots are silty clay in SCS, and the purple ▲ is clayey silt in WP.

Table 2 list the values of Biot–Stoll model input parameters for different sediment types, including silty sand, silt, silty clay sediment in SCS, and clayey silt sediment in WP. Figure 5 shows the best Biot–Stoll model fit sound speed predictions for different sediments in SCS. The silty sand has highest sound speed and the inflection point from low frequency to high frequency is more obvious. In general, coarse particles have significant sound speed dispersion and the inflection point is located in the low frequency band, while fine particles have weak sound speed dispersion and the inflection point is located in the high-frequency band. Figure 5 shows that the sound speed and attenuation inflection point of coarse grain sediment is obvious and low in frequency (silty sand), while that of fine grain sediment is not obvious and high in frequency (silty clay). Williams et al. [1] studied the uncertainty in model predictions given the uncertainty for the measured physical parameters, and their result shows that the permeability and tortuosity uncertainties result in the largest model attenuation uncertainties, and for sound speed, the permeability affects the sound speed dispersion in the middle-frequency range, and the tortuosity affects the sound speed dispersion in the high-frequency range. For attenuation, the permeability affects the whole frequency range, whereas the tortuosity affects the >1 kHz frequency range. In the Figure 1 of Williams et al. [1], the sound speed dispersion inflection point is influenced by the permeability parameter; in this study, the permeability of silty sand is  $2.25 \times 10^{-11}$  and the silty clay is only  $2.14 \times 10^{-12}$ ; the three sediments in SCS also showed that, the higher permeability is, the lower the frequency of the sound speed and attenuation dispersion inflection point.

**Table 2.** The values of Biot–Stoll model input parameters for different sediment types.

Physical Parameter	Symbol	Unit	South China Sea Silty Sand	South China Sea Silt	South China Sea Silty Clay	Western Pacific Clayey Silt
Porosity	$n$	-	0.482	0.550	0.694	0.663
Mean grain size	$Mz$	$\phi$	3.19	5.01	6.58	6.98
Grain bulk modulus *	$K_g$	Pa	$3.6 \times 10^{10}$	$3.6 \times 10^{10}$	$3.6 \times 10^{10}$	$3.6 \times 10^{10}$
Fluid dynamic viscosity *	$\eta$	$\text{kg}\cdot\text{m}^{-1}\cdot\text{s}^{-1}$	0.00105	0.00105	0.00105	0.00105
Grain density	$\rho_g$	$\text{kg}\cdot\text{m}^{-3}$	2650	2650	2650	2650
Fluid density *	$\rho_f$	$\text{kg}\cdot\text{m}^{-3}$	1023	1023	1023	1023
Fluid bulk modulus *	$K_f$	Pa	$2.23 \times 10^9$	$2.23 \times 10^9$	$2.23 \times 10^9$	$2.23 \times 10^9$
Permeability +	$\kappa$	$\text{m}^2$	$2.25 \times 10^{-11}$	$4.38 \times 10^{-12}$	$2.14 \times 10^{-12}$	$8.89 \times 10^{-13}$
Tortuosity +	$\alpha$	—	1.35	1.76	2.41	2.58
Pore size +	$a$	m	$2.49 \times 10^{-5}$	$1.01 \times 10^{-5}$	$6.27 \times 10^{-6}$	$4.13 \times 10^{-6}$
Frame shear modulus *	$\mu$	Pa	$(1.178 - i0.18) \times 10^7$	$(0.725 - i0.18) \times 10^7$	$(0.299 - i0.18) \times 10^7$	$(0.368 - i0.18) \times 10^7$
Frame bulk modulus *	$K_b$	Pa	$(1.532 - i0.24) \times 10^7$	$(0.943 - i0.20) \times 10^7$	$(0.389 - i0.24) \times 10^7$	$(0.479 - i0.20) \times 10^7$

The symbol (\*) indicates estimated parameters from the literature. The symbol (+) indicates the calculated parameter using measured parameters. The calculation of permeability, tortuosity, and pore size can be seen in [20], Formulas (3) to (6).



**Figure 5.** The sound speed (a) and attenuation (b) dispersion of different sediments in SCS.

Figure 6 shows the comparison of different sediments from different areas. The blue line is the coarse sand sediment measured during the sediment acoustics experiment in 1999 (SAX99) by Williams et al. [1], and the measurements span the frequency range of about 125 Hz–400 kHz, and the permeability of the coarse sand is  $2.5 \times 10^{-11}$ . The red line is the fine sand sediment measured in the East China Sea shelf [21], with a frequency range of 30–87 kHz, including the in situ data with the measured frequency of 30 kHz, and the sediment core measurement data with the frequencies range of 47–87 kHz, and the permeability of the fine sand is  $3.77 \times 10^{-12}$ . The green line is the sandy silt sediment measured in Currituck Sound, North Carolina [22], the compressional wave sound speed and attenuation were measured in the frequency band of 5–100 kHz, and the permeability of the sandy silt is  $8.5 \times 10^{-12}$ . The purple line is the clayey silt sediment in WP measured at the frequencies of 27, 51, 111, 214, and 247 kHz, respectively, (unpublished), and the permeability of the clayey silt is  $8.9 \times 10^{-13}$ . In Figure 6, the dispersion inflection point is closely related with the permeability, and it confirmed that the higher permeability is, the lower the frequency of the sound speed and attenuation dispersion inflection point.

In Figure 6, the attenuations of coarse sand and silty sand are the greatest attenuations in the low-frequency band (<10 kHz). However, as the frequency increased, the attenuation of coarse sand and silty sand sediment become lowest in the high-frequency band (>10 kHz).

By contrast, the silty clay and clayey silt sediments have low attenuation in the low-frequency band (<10 kHz) and become high as the frequency increases. In the low-frequency band, the sound speed ratio of silt and clayey silt is similar, while in the high-frequency band, the sound speed ratio of silt and is obviously higher than that of clayey silt, which is because at the high frequency, silt and clayey silt have almost equal sound attenuation, while the sound speed of silt is higher than that of clayey silt.

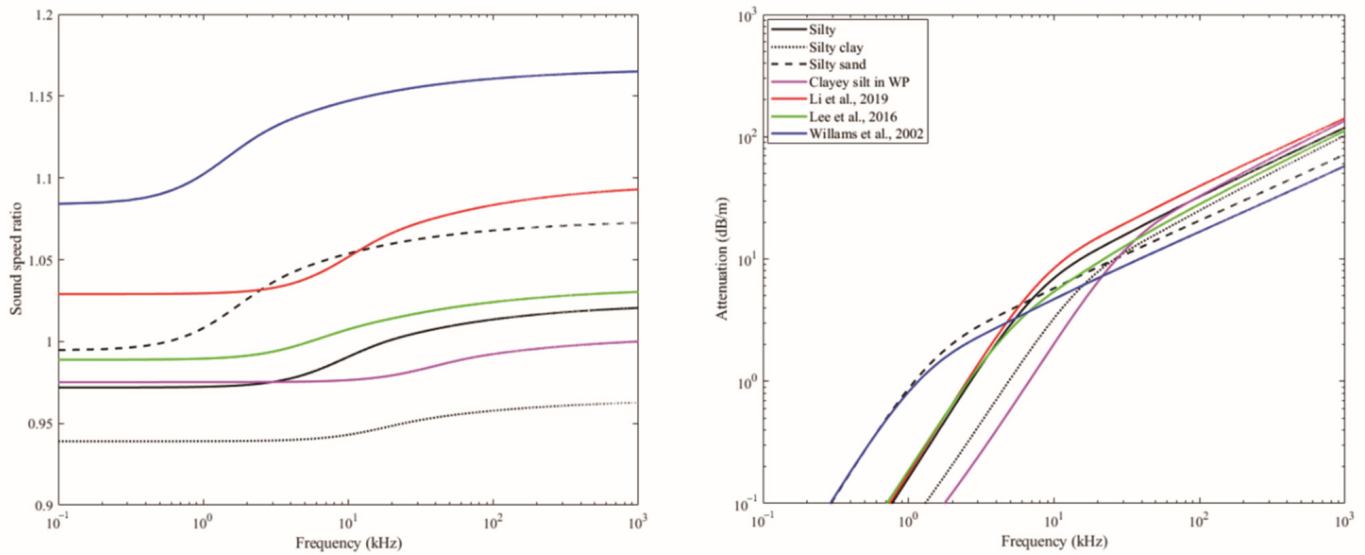


**Figure 6.** The sound speed and attenuation dispersion for different area and sediment types. The blue line is coarse sand [1], The red line is fine sand [21], the green line is sandy silt [22], and the purple line is clayey silt in WP.

In sound speed dispersion curve, coarse sand [1] and silty sand (SCS) have obvious differences with the other four kinds of sediment; because of their high permeability, the dispersion inflection point of coarse sand and silty sand occurs at lower frequencies than the other four kinds of sediment. As the attenuation of coarse sand and silty sand is the largest at the low-frequency band, the low-frequency dispersion curve of coarse sand and silty sand has a certain radian, while the other four kinds of sediment are basically parallel to the coordinate axis at low frequency, and the variation of the low-frequency dispersion is small.

#### 4. Conclusions

In this paper, historical data of acoustic properties of seafloor sediments in the SCS are collected, and three typical types (silty clay, silt, and silty sand) of sediments are selected to carry out high-frequency-dependence (27, 51, 111, 214, and 247 kHz, respectively) characteristic analysis, and established the relation between sound speed and attenuation dispersion of fine sediment. The frequency dispersion of the three sediments were modeled by the Biot–Stoll model and compared with different sediments from different literatures.

(1) The dispersion curves of the SCS and WP sediments are almost parallel, and the frequency dispersion degree of the four sediments is 1.0687% (silty clay), 1.0121% (clayey silt), 1.22% (silt), and 1.5529% (silty sand), respectively.

(2) The sound speed dispersion of different sediments at the frequency of 27–247 kHz:  
 $C_p = 0.0956f + 1609.5$  (silty sand);  $C_p = 0.0759f + 1545.6$  (silt);  $C_p = 0.0614f + 1499.6$  (clayey silt);  $C_p = 0.0658f + 1450.6$  (silty clay).

The attenuation dispersion of different sediments at the frequency of 27–247 kHz:  
 $\alpha = 1.5933f^{0.68}$  (silty sand);  $\alpha = 1.5231f^{0.59}$  (silt);  $\alpha = 6.4178f^{0.35}$  (clayey silt);  $\alpha = 0.2831f^{0.87}$  (silty clay).

(3) The inflection point of frequency dispersion is different for different types of sediments. Permeability is the key parameter that determines the inflection point of high frequency to low frequency. In this study, the sound speed dispersion degree of three kinds of sediments in SCS: silty sand > silt > silty clay, and silty sand has the earliest inflection point.

In the low-frequency band, sound attenuation varies greatly, the coarse sand [1] and silty sand (SCS) have the highest attenuation, and clayey silt (WP) has the lowest attenuation. In the high-frequency band, the variation of attenuation is small, and the attenuation coefficients of these sediments are basically parallel. The largest attenuation is fine sand [19], and the smallest attenuation is coarse sand [1].

**Author Contributions:** Conceptualization, J.W. and Z.H.; methodology, J.W. and Z.H.; validation, G.L., G.K., X.M., B.L. and L.S.; formal analysis, Z.H.; investigation, J.W., G.L., G.K., X.M., Q.H. and L.S.; data curation, J.W. and Z.H.; writing—original draft preparation, Z.H.; writing—review and editing, J.W. and Z.H.; visualization, J.W.; supervision, B.L.; project administration, J.W. and Z.H.; funding acquisition, J.W. and Z.H. All authors have read and agreed to the published version of the manuscript.

**Funding:** This study was supported by the National Key R&D Program of China (2021YFF0501202), Basic Scientific Fund for National Public Research Institutes of China (2022S01), the National Natural Science Foundation of China under contracts Nos. 42176191, the National Key Laboratory of Science and Technology on Underwater Acoustic Antagonizing, Youth Innovation Promotion Association CAS, the Rising Star Foundation of The Integrated Research Center For Islands And Reefs Sciences, CAS (ZDRW-XH-2021-2-03), the Taishan Scholar Project Funding under contract No. tspd20161007, the CAS Key Laboratory of Science and Technology on Operational Oceanography Open Project Funding No OOST2021-01.

**Institutional Review Board Statement:** Not applicable.

**Informed Consent Statement:** Not applicable.

**Data Availability Statement:** Not applicable.

**Acknowledgments:** We thank the associate editor and the reviewers for their useful feedback that improved this paper.

**Conflicts of Interest:** The authors declare no conflict of interest.

## References

1. Williams, K.L.; Jackson, D.R.; Thorsos, E.I.; Tang, D.; Schock, S.G. Comparison of sound velocity and attenuation measured in a sandy sediment to predictions based on the Biot theory of porous media. *IEEE J. Ocean. Eng.* **2002**, *27*, 413–428. [[CrossRef](#)]
2. Guo, X.S.; Stoesser, T.; Nian, T.K.; Jia, Y.G.; Liu, X.L. Effect of pipeline surface roughness on peak impact forces caused by submarine mudflow. *Ocea. Eng.* **2022**, *243*, 110184. [[CrossRef](#)]
3. Gassmann, F. Über die Elastizität poröser Medien (Elasticity of porous media. *Vierteljahrsschrift der Naturforschenden. Gesellschaft Zur.* **1951**, *96*, 1–23.
4. Biot, M.A. Theory of propagation of elastic waves in a fluid-saturated porous solid. II. Higher frequency range. *J. Acoust. Soc. Am.* **1956**, *28*, 179–191. [[CrossRef](#)]
5. Hamilton, E.L. Geoacoustic modeling of the sea floor. *J. Acoust. Soc. Am.* **1980**, *68*, 1313–1340. [[CrossRef](#)]
6. Stoll, R.D.; Kan, T.K. Reflection of acoustic waves at a water-sediment interface. *J. Acoust. Soc. Am.* **1981**, *28*, 149–156. [[CrossRef](#)]
7. Williams, K.L. An effective density fluid model for acoustic propagation in sediments derived from Biot theory. *J. Acoust. Soc. Am.* **2001**, *110*, 2276–2281. [[CrossRef](#)] [[PubMed](#)]
8. Jackson, D.R.; Richardson, M.D. *High-frequency Seafloor Acoustics*; Springer Science + Business Media: New York, NY, USA, 2007.
9. Hovem, J.M.; Ingram, G.D. Viscous attenuation of sound in saturated sand. *J. Acoust. Soc. Am.* **1979**, *66*, 1807–1812. [[CrossRef](#)]
10. Simpson, H.J.; Houston, B.H.; Liskey, S.W.; Frank, P.A.; Berdoz, A.R.; Kraus, L.A.; Frederickson, C.K.; Stanic, S. At-sea measurements of sound penetration into sediments using a buried vertical synthetic array. *J. Acoust. Soc. Am.* **2003**, *114*, 1281–1290. [[CrossRef](#)] [[PubMed](#)]
11. Ragione, L.L.; Recchia, G.; Jenkins, J.T. Wave propagation in an unconsolidated granular material: A micro-mechanical approach. *Wave Motion* **2020**, *99*, 102653. [[CrossRef](#)]
12. Buckingham, M.J. On pore-fluid viscosity and the wave properties of saturated granular materials including marine sediments. *J. Acoust. Soc. Am.* **2007**, *122*, 1486. [[CrossRef](#)] [[PubMed](#)]

13. Bonomo, A.L.; Isakson, M.J. A comparison of three geoacoustic models using Bayesian inversion and selection techniques applied to wave speed and attenuation measurements. *J. Acoust. Soc. Am.* **2018**, *143*, 2501–2513. [[CrossRef](#)]
14. Holmes, J.D.; Carey, W.M.; Dediu, S.M.; Siegmann, W.L. Nonlinear frequency-dependent attenuation in sandy sediments. *J. Acoust. Soc. Am.* **2007**, *121*, EL218–EL222. [[CrossRef](#)] [[PubMed](#)]
15. Sessarego, J.P.; Ivakin, A.N.; Ferrand, D. Frequency Dependence of Phase Speed, Group Speed, and Attenuation in Water-Saturated Sand: Laboratory Experiments. *IEEE J. Ocean. Eng.* **2009**, *33*, 359–366. [[CrossRef](#)]
16. Yu, S.; Wang, F.; Zheng, G.; Huang, Y. Progress and discussions in acoustic properties of marine sediments. *J. Harbin Eng. Univ.* **2020**, *41*, 7.
17. Hamilton, E.L. Compressional wave attenuation in marine sediments. *Geophysics.* **1972**, *37*, 620–646. [[CrossRef](#)]
18. Hou, Z.; Chen, Z.; Wang, J.; Zheng, X.; Yan, W.; Tian, Y.; Luo, Y. Acoustic characteristics of seafloor sediments in the abyssal areas of the South China Sea. *Ocea. Eng.* **2018**, *156*, 93–100. [[CrossRef](#)]
19. Stoll, R.D. *Sediment Acoustics*; Springer: Berlin/Heidelberg, Germany, 1989.
20. Wang, J.; Li, G.; Kan, G.; Hou, Z.; Meng, X.; Liu, B.; Liu, C.; Lei, S. High frequency dependence of sound speed and attenuation in coral sand sediments. *Ocea. Eng.* **2021**, *234*, 109215. [[CrossRef](#)]
21. Li, G.; Wang, J.; Liu, B.; Meng, X.; Kan, G.; Pei, Y. Measurement and modeling of high-frequency acoustic properties in fine sandy sediments. *Earth Space Sci.* **2019**, *6*, 2057–2070. [[CrossRef](#)]
22. Lee, K.M.; Ballard, M.S.; Mcneese, A.R.; Muir, T.G.; Wilson, P.S.; Costley, R.D.; Hathaway, K.K. In situ measurements of sediment acoustic properties in Currituck Sound and comparison to models. *J. Acoust. Soc. Am.* **2016**, *140*, 3593. [[CrossRef](#)] [[PubMed](#)]